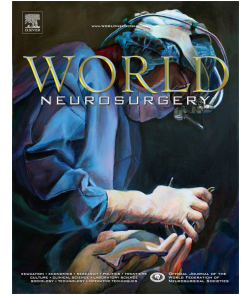


# Journal Pre-proof

Impaired dynamic cerebral autoregulation as a predictor for cerebral hyperperfusion after carotid endarterectomy: A prospective observational study

Na Li, Fubo Zhou, Xia Lu, Hongxiu Chen, Ran Liu, Songwei Chen, Yingqi Xing



PII: S1878-8750(23)01451-1

DOI: <https://doi.org/10.1016/j.wneu.2023.10.046>

Reference: WNEU 21277

To appear in: *World Neurosurgery*

Received Date: 20 August 2023

Revised Date: 8 October 2023

Accepted Date: 8 October 2023

Please cite this article as: Li N, Zhou F, Lu X, Chen H, Liu R, Chen S, Xing Y, Impaired dynamic cerebral autoregulation as a predictor for cerebral hyperperfusion after carotid endarterectomy: A prospective observational study, *World Neurosurgery* (2023), doi: <https://doi.org/10.1016/j.wneu.2023.10.046>.

This is a PDF file of an article that has undergone enhancements after acceptance, such as the addition of a cover page and metadata, and formatting for readability, but it is not yet the definitive version of record. This version will undergo additional copyediting, typesetting and review before it is published in its final form, but we are providing this version to give early visibility of the article. Please note that, during the production process, errors may be discovered which could affect the content, and all legal disclaimers that apply to the journal pertain.

© 2023 Published by Elsevier Inc.

1 **Impaired dynamic cerebral autoregulation as a predictor for cerebral hyperperfusion**  
2 **after carotid endarterectomy: A prospective observational study**

3

4 Na Li<sup>1, 2, 3</sup>; Fubo Zhou<sup>1, 2, 3</sup>; Xia Lu<sup>4</sup>; Hongxiu Chen<sup>1, 2, 3</sup>; Ran Liu<sup>1, 2, 3</sup>; Songwei Chen<sup>1, 2, 3</sup>;  
5 Yingqi Xing<sup>1, 2, 3, \*</sup>

6

7 Affiliations:

8 <sup>1</sup> Department of Vascular Ultrasonography, Xuanwu Hospital, Capital Medical University,  
9 Beijing, China

10 <sup>2</sup> Beijing Diagnostic Center of Vascular Ultrasound, Beijing, China

11 <sup>3</sup> Center of Vascular Ultrasonography, Beijing Institute of Brain Disorders, Collaborative  
12 Innovation Center for Brain Disorders, Capital Medical University, Beijing, China

13 <sup>4</sup> Department of Neurosurgery, Xuanwu Hospital, Capital Medical University, Beijing, China

14

15 Na Li (MD)

16 Email: [krb1119@163.com](mailto:krb1119@163.com)

17 Phone number: +86 15910916123

18

19 Fubo Zhou (MD, PhD)

20 Email: [myzhoufubo@126.com](mailto:myzhoufubo@126.com)

21 Phone number: +86 13520481689

22

23 Xia Lu (MD, PhD)

24 Email: [luxia@xwhosp.org](mailto:luxia@xwhosp.org)

25 Phone number: +86 01083198435

26

27 Hongxiu Chen (MD)

28 Email: [1219634275@qq.com](mailto:1219634275@qq.com)

29 Phone number: +86 18001366163

30

31 Ran Liu (MD)

1 Email: [winglsw@126.com](mailto:winglsw@126.com)

2 Phone number: +86 13552322523

3

4 Songwei Chen (MD)

5 Email: [csw1021@sina.com](mailto:csw1021@sina.com)

6 Phone number: +86 15896921765

7

8

9 \*Corresponding author:

10 Yingqi Xing (MD, PhD)

11 Department of Vascular Ultrasonography,

12 Xuanwu Hospital, Capital Medical University, No. 45, Changchun Street, Xicheng District

13 Beijing, 100053, China

14 Email: [xingyq2009@sina.com](mailto:xingyq2009@sina.com)

15 Phone number: +86 18610047846

16

17 Running title: Predictive utility of dCA for CH after CEA

18

19 **Keywords :** Carotid endarterectomy, cerebral autoregulation, cerebral hyperperfusion,  
20 hemodynamics, Transcranial Doppler Ultrasound

1 **Impaired dynamic cerebral autoregulation as a predictor for cerebral hyperperfusion**  
2 **after carotid endarterectomy: A prospective observational study**

3

4 **Abstract**

5 **Objective:** Cerebral hyperperfusion syndrome (CHS) is a severe complication of carotid  
6 endarterectomy (CEA). Because cerebral hyperperfusion (CH) reduces the benefits of CEA,  
7 it is important to identify patients at high risk of developing CH. We investigated dynamic  
8 cerebral autoregulation (dCA) as a potential predictor of CH after CEA.

9 **Methods:** In a prospective observational study of 90 patients, we defined CH as a  $\geq 100\%$   
10 increase in the transcranial Doppler ultrasound-derived mean flow velocity of the middle  
11 cerebral artery compared to baseline, with or without clinical manifestations. We examined  
12 dCA in the supine position and during squat-stand maneuvers using the transfer function,  
13 analyzing phase, gain, and coherence. Logistic regression analysis and receiver operating  
14 characteristic curves were used to assess the relationships between variables and outcomes.

15 **Results:** CH occurred in 18 patients after CEA. The CH group had a lower ipsilateral phase  
16 for both body postures than the non-CH group at very low and low frequencies, respectively  
17 (both  $P < 0.01$ ). Postoperative CH was independently associated with the preoperative peak  
18 systolic velocity (PSV)<sub>sten</sub>/PSV<sub>dis</sub> ratio and the ipsilateral phase in both body postures at a  
19 very low frequency. Receiver operating characteristic curve analysis showed that the  
20 ipsilateral phase had excellent CH predictive accuracy in the supine position and squat-stand  
21 maneuvers at a very low frequency (areas under the curve: 0.809 and 0.839, respectively,  
22 both  $P < 0.001$ ; cutoff values: 24.7 and 11.7, respectively).

23 **Conclusions:** The lower ipsilateral phase may serve as a predictor of CH after CEA.

24

25 **Keywords:** Carotid endarterectomy, Cerebral autoregulation, Cerebral hyperperfusion,

26 Hemodynamics, Transcranial Doppler Ultrasound

27

## 28 **Introduction**

29 Atherosclerotic stenosis of the carotid artery is a major cause of ischemic stroke. Carotid  
30 endarterectomy (CEA) is considered the standard treatment for reducing the risk of stroke in  
31 patients with severe carotid stenosis. Cerebral hyperperfusion (CH) is defined as an excessive  
32 increase in ipsilateral cerebral blood flow (CBF) relative to metabolic needs following carotid  
33 revascularization.<sup>1</sup>

34 Cerebral hyperperfusion syndrome (CHS) is a rare but important perioperative  
35 complication of CEA. It is characterized by an ipsilateral headache, eye and face pain,  
36 vomiting, seizures, focal neurological deficits, and intracranial hemorrhage (ICH).<sup>1-3</sup>

37 Although the reported incidence of CHS is 1%–3%, the morbidity and mortality rates among  
38 patients with CHS who present with ICH are as high as 50%.<sup>1,4</sup> CHS often occurs in patients  
39 with CH.<sup>5</sup> Given that CHS reduces the benefits of CEA, especially among patients with  
40 asymptomatic carotid disease, it is important to identify patients at a high risk of developing  
41 CHS.

42 Impaired cerebrovascular autoregulation is crucially involved in CH.<sup>2</sup> Dynamic cerebral  
43 autoregulation (dCA) refers to the ability to adapt cerebral vasoconstriction and vasodilation  
44 according to blood pressure (BP) fluctuations within a certain range to regulate and stabilize  
45 CBF.<sup>6</sup> As the brain is highly dependent on the continuous supply of oxygenated blood,  
46 reduced effectiveness of dCA increases the brain's sensitivity to hypoperfusion and  
47 hyperperfusion.<sup>7</sup> Transfer function analysis (TFA), the most widely used dCA monitoring

48 method, has been employed to study ischemic stroke, ICH, and neurodegeneration, among  
49 other diseases.<sup>8-10</sup> However, few studies have used TFA to investigate CEA.

50       Ultrasound combined with transcranial Doppler ultrasound (TCD) provides information  
51 regarding hemodynamics and dCA. TCD is a reliable tool to identify post-reperfusion  
52 hyperperfusion and correlates with perfusion magnetic resonance (MR) imaging.<sup>11</sup> Moreover,  
53 preoperative hemodynamics and dCA may be useful imaging markers for clinically  
54 predicting CHS. Therefore, this study investigated the utility of impaired dCA as a potential  
55 predictor of CH after CEA.

56

## 57 **Methods**

### 58 *Research participants*

59       This study was approved by the Ethics Committee of the Capital Medical University  
60 Xuanwu Hospital (approval number [2019]073). All experimental procedures were performed  
61 following the principles of the Declaration of Helsinki. Written informed consent was  
62 obtained from all participants.

63       We prospectively included 90 consecutive patients who underwent CEA at Xuanwu  
64 Hospital, Capital Medical University, China, between March 2021 and September 2022. The  
65 inclusion criteria were as follows: (1) Severe (70–99%) unilateral carotid artery stenosis  
66 diagnosed by duplex ultrasound and confirmed by computed tomography angiography (CTA)  
67 or digital subtraction angiography (DSA) based on the criteria used in the North American  
68 Symptomatic Carotid Endarterectomy Trial,<sup>12</sup> and (2) age of 18–80 years. The exclusion  
69 criteria were as follows: (1) CEA performed for non-atherosclerotic diseases; (2) severe  
70 stenosis (70%–99%) or occlusion of the contralateral carotid artery, bilateral subclavian  
71 artery, and/or vertebrobasilar artery; (3) moderate or higher-grade stenosis of the unilateral or  
72 bilateral middle cerebral artery (MCA); (4) hybrid operation or unsuccessful carotid

73 revascularization; (5) poor temporal window prohibitive of TCD monitoring; and (6) heart  
74 failure, congenital heart disease, severe cardiac arrhythmia, acute or chronic infection, or  
75 other serious systemic diseases. Figure 1 represents a flow chart of patient enrollment.

76

### 77 *Carotid artery ultrasound and transcranial color code sonography*

78 All patients underwent preoperative duplex ultrasound evaluation of the carotid artery  
79 and MCA by sufficiently trained doctors with > 5 years of experience in vascular ultrasound.  
80 This assessment was performed using a Hitachi Ascendus (Hitachi, Inc., Tokyo, Japan)  
81 ultrasound instrument with a 4.0–8.0 MHz micro curvilinear transducer, 2.0–5.0 MHz convey  
82 array probes, and 1.0–5.0 MHz phased array probes. While measuring carotid velocity, the  
83 angle between the ultrasound beam and blood flow was set to  $\leq 60^\circ$ . The MCA velocity was  
84 measured at  $< 30^\circ$ . All acquired images were stored in a picture archiving and communication  
85 system for subsequent analyses.

86 The imaging parameters were as follows: (1) peak systolic velocity ( $PSV_{sten}$ ) and end  
87 diastolic velocity ( $EDV_{sten}$ ) at the carotid stenosis; (2) peak systolic velocity ( $PSV_{dis}$ ) and end  
88 diastolic velocity ( $EDV_{dis}$ ) at 4–6 cm beyond the carotid bifurcation; and (3) PSV, diastolic  
89 velocity, and pulsatility index (PI) of the ipsilateral ( $PI_{oper}$ ) and contralesional ( $PI_{con}$ ) MCA  
90 before CEA. Subsequently, we calculated the ratios  $PSV_{sten}/PSV_{dis}$  and  $PI_{con}/PI_{oper}$ .

91

### 92 *Study protocol/dCA measurement*

93 All dCA data were collected in an environmentally controlled laboratory (22°C–24°C)  
94 with non-sensory stimuli (e.g., noise, lights) controlled based on the international white paper  
95 of cerebral autoregulation assessments.<sup>7</sup> Participants were asked to refrain from nicotine,  
96 caffeine, chocolate, and alcohol consumption for at least 12 h and high calorie meals for at  
97 least 4 h before the study. Furthermore, participants were asked to refrain from moderate-

98 vigorous exercise for at least 6 h prior to measurement. After lying down at rest for 15 min  
99 with uncrossed legs, the examination was started.

100 Participants were fitted with a head frame. Continuous cerebral blood flow velocity  
101 (CBFV) was measured in the bilateral MCA at a depth of 50–65 mm through the temporal  
102 window with 1.6 MHz ultrasound probes using TCD (EMS-9D Pro; Delica Medical,  
103 Shenzhen, China). We recorded non-invasive continuous beat-to-beat BP (NIBP) using a  
104 servo-controlled plethysmograph (Finometer; Enschede, Netherlands) attached to the finger.  
105 Before each NIBP measurement, brachial BP was measured using a sphygmomanometer  
106 (Omron HBP-1300; Kyoto, Japan) to calibrate the baseline BP signal. The sampling  
107 frequency of the Doppler trace and NIBP signal was 125 Hz.<sup>13</sup> The heart rate was measured  
108 via four-lead electrocardiography. Respiratory rate and end-tidal carbon dioxide (Et-CO<sub>2</sub>)  
109 during spontaneous breathing were recorded using a nasal cannula with a nasal capnograph.

110  
111 *Baseline.* Once satisfactory signals were obtained from all equipment, we obtained the  
112 baseline brachial BP, heart rate, and Et-CO<sub>2</sub> measurements within a 10-min period with the  
113 participants in the supine position while breathing room air.

114  
115 *Squat-stand maneuvers (SSMs).* After standing for 2 min, the participants performed a  
116 maximum of 15 SSMs at a 0.05-Hz frequency (standing for 10 s, squatting for 10 s). The  
117 squats involved bending the knees at 45° for 10 s, followed by standing straight for another  
118 10 s.<sup>14</sup> A voice prompt provided by a computer program was used to ensure that the SSMs  
119 were performed at the standard frequency. A highchair was placed in front of the participants,  
120 which they could lightly touch to maintain balance if required. A bed was set at the correct  
121 height behind the participants to guide the depth of each squat; moreover, participants were  
122 instructed not to place any weight on the bed.<sup>15</sup> Throughout each recording, the participants



123 were asked to breathe through their noses and avoid Valsalva-like maneuvers during the  
124 SSMs. Verbal communication was avoided during data collection. After the SSMs, the  
125 participants were placed in the supine position for 2 min (Figure 2).

126

### 127 *dCA analysis*

128 Cerebral autoregulation parameters were calculated based on TFA,<sup>7</sup> with NIBP and  
129 CBFV as the input and output signals, respectively. TFA is based on the Fourier  
130 decomposition of stationary input and output signals into the sums of sines and cosines of  
131 multiple frequencies. The transfer function estimates of the dCA metrics were calculated at  
132 very low frequency (VLF, 0.02–0.07 Hz), low frequency (LF, 0.07–0.20 Hz), and high  
133 frequency (HF, 0.20–0.50 Hz), with gain, phase, and coherence parameters.<sup>16</sup> This phase shift  
134 represented the time delay of the CBFV response to NIBP. The gain represented the damping  
135 effect of dCA on the magnitude of BP oscillations. Coherence helped to identify conditions in  
136 which estimates of gain and phase may be unreliable. We only estimated dCA parameters if  
137 the coherence was  $> 0.5$ .

138

### 139 *CEA*

140 CEA was performed under general anesthesia, with all patients administered the same  
141 anesthetic regimen. All CEA procedures were performed by experienced vascular surgeons.  
142 Conventional CEA was performed as previously described.<sup>17</sup> Throughout the operation,  
143 patients were monitored using TCD (EMS-9PB, Delica, Shenzhen, China) and routine  
144 electrocardiographic monitoring. CH was defined as an intraoperative increase in the TCD-  
145 derived mean flow velocity in the middle cerebral artery ( $MCAV_{mean}$ ) by  $\geq 100\%$  after carotid  
146 de-clamping compared with baseline  $MCAV_{mean}$  from de-clamping to suturing, regardless of  
147 clinical manifestations. CHS was defined as CH combined with clinical symptoms such as

148 headache, confusion, seizures, ICH, or focal neurological deficits, following a symptom-free  
149 interval.<sup>18</sup>

150

### 151 *Other clinical and imaging characteristics*

152 We collected patients' demographic and clinical data, including age, sex, height, and  
153 weight; neurological and cardiovascular history; and vascular risk factors, including  
154 hypertension, diabetes mellitus, dyslipidemia, smoking history, and alcohol consumption. In  
155 case the anterior communicating artery and/or posterior communicating artery were visible  
156 on computed tomography angiography or MR angiography, this was defined as the "presence  
157 of primary collaterals." Additionally, we recorded the patients' clinical symptoms and  
158 preoperative and postoperative brain MR imaging findings.

159

### 160 *Statistical analysis*

161 Statistical analyses were performed using SPSS Statistical Software 22.0 (IBM  
162 Corporation, Armonk, NY, USA) and MedCalc version 19.6.1 (MedCalc Software, Ostend,  
163 Belgium). All continuous variables were tested for normal distribution using the Shapiro–  
164 Wilk test, with normally and non-normally distributed variables expressed as mean  $\pm$   
165 standard deviation and median (interquartile range), respectively. Categorical variables are  
166 presented as n (%). Between-group comparisons of normally and non-normally variables  
167 were performed using the independent Student t-test or Mann–Whitney U-test, respectively.  
168 The chi-square test was used for between-group comparisons of categorical variables.  
169 Multivariate analysis was conducted using a logistic regression model, including factors with  
170  $P < 0.10$  in the univariate analysis. Receiver operating characteristic (ROC) curve analysis  
171 was performed to identify the cutoff value. The area under the curve (AUC), optimal cutoff  
172 value, sensitivity, and specificity were calculated. ROC curves were compared using

173 DeLong's test. A two-sided  $P < 0.05$  was considered statistically significant and confidence  
174 intervals (CIs) were set at 95%.

175

## 176 **Results**

### 177 *Characteristics of the study population*

178 We included 90 patients in the study (82 men and 8 women; mean age:  $63.1 \pm 7.6$  years  
179 [range, 37–80 years]). CEA was successfully performed in all patients. Table 1 presents the  
180 baseline demographic characteristics, clinical data, and laboratory test results of the CH ( $n =$   
181 18) and non-CH ( $n = 72$ ) groups. There were no significant between-group differences  
182 regarding demographics, vascular risk factors, or laboratory indices. Regarding hemodynamic  
183 parameters, the  $PSV_{sten}/PSV_{dis}$  was higher in the CH group than in the non-CH group ( $P <$   
184 0.001).

185

### 186 *dCA parameters in the CH and non-CH groups in the supine position and during SSMS*

187 Table 2 and Table 3 show the dCA values in both groups during the supine position and  
188 SSMS. The CH group had a lower ipsilateral phase degree than the non-CH group during the  
189 supine position and SSMS in both the VLF and LF ranges (all  $P < 0.01$ ) but not in the HF  
190 range. Additionally, there were no significant differences in the gain and absolute gain  
191 between the supine position and SSMS ( $P > 0.05$ ). Squat-stand maneuvers showed higher  
192 coherence than supine maneuvers in all patients in the very low and low frequency range (all  
193  $P < 0.001$ ); however, there was no significant difference in the high frequency range ( $P =$   
194 0.904).

195

### 196 *Multivariate analysis*

197  $PSV_{sten}/PSV_{dis}$  (adjusted odds ratio [aOR]: 1.114, 95% CI: 1.029–1.206,  $P = 0.008$ ),

198 ipsilateral phase (supine) at the VLF (aOR: 0.938, 95% CI: 0.894–0.985,  $P = 0.01$ ), and  
199 ipsilateral phase (SSMs) at the VLF (aOR: 0.929, 95% CI: 0.877–0.985,  $P = 0.013$ ) were  
200 identified as independent predictors of CH after CEA.

201

### 202 *Comparison of ROC curves*

203 We compared the ROC curves of four models. Model 1 comprised only the ipsilateral  
204 phase (supine) at the VLF; Model 2 comprised the ipsilateral phase (SSMs) at the VLF;  
205 Model 3 comprised a combination of Model 1 with the  $PSV_{sten}/PSV_{dis}$  ratio; Model 4  
206 comprised a combination of Model 2 and  $PSV_{sten}/PSV_{dis}$  ratio. For Models 1, 2, 3, and 4, the  
207 AUCs were 0.809 (95% CI: 0.712–0.884), 0.839 (95% CI: 0.746–0.908), 0.883 (95% CI:  
208 0.799–0.942), and 0.869 (95% CI: 0.781–0.931), respectively, with no significant between-  
209 model differences ( $P = 0.119$  for Model 1 vs. Model 3;  $P = 0.272$  for Model 2 vs. Model 4)  
210 (Figure 3). The optimal cutoff phase value used to distinguish patients with and without CH  
211 was obtained based on the maximum Youden index. The optimal cutoff values of the  
212 ipsilateral phase (supine) and ipsilateral phase (SSMs) at the VLF for predicting CH were  $\leq$   
213 24.7 and  $\leq 11.7$ , respectively. The proportion of patients with CH in the ipsilateral phase  
214 (supine)  $\leq 24.7$  group was significantly higher than that in the ipsilateral phase (supine)  $>$   
215 24.7 group (50.0% vs. 5.0%,  $P < 0.001$ ). Furthermore, the proportion of patients with CH in  
216 the ipsilateral phase (SSMs)  $\leq 11.7$  group was significantly higher than that in the ipsilateral  
217 phase (SSMs)  $> 11.7$  group (68.4% vs. 7.0%,  $P < 0.001$ ) (Figure 4).

218

### 219 **Discussion**

220 This single-center prospective study explored the relationship of hemodynamic or dCA  
221 parameters of CH after CEA in patients with carotid stenosis. We found that higher  
222  $PSV_{sten}/PSV_{dis}$  ratios and lower ipsilateral phase degrees were strongly associated with CH

223 after CEA. Moreover, the ipsilateral phase (supine) and ipsilateral phase (SSMs) in the VLF  
224 showed high predictive utility for CH after CEA, which did not increase with the inclusion of  
225 the  $PSV_{sten}/PSV_{dis}$  ratio. This finding demonstrates the predictive utility of dCA for CH after  
226 CEA, with high sensitivity and specificity.

227 Impaired cerebral autoregulation is the most widely accepted mechanism contributing to  
228 the development of CHS.<sup>1</sup> Chronic severe carotid stenosis leads to chronic brain ischemia.  
229 The arterioles and capillaries of patients with dysfunctional cerebral autoregulation are more  
230 vulnerable to rupture and bleeding upon an abrupt increase in perfusion pressure following  
231 revascularization.<sup>2</sup> We used TFA to analyze the dCA. The phase degree (supine) in both the  
232 VLF and LF ranges was lower in the CH group than in the non-CH group. This result  
233 suggests that patients with CH have more severely impaired dCA than patients without CH.  
234 Furthermore, we compared differences in the dCA during the supine position and SSMs. The  
235 phases in the VLF and LF ranges were markedly lower in the CH group than in the non-CH  
236 group. Regarding SSMs, the large oscillations in evoked BP were transmitted to cerebral  
237 perfusion, which increased the coherence between these variables and optimizes the TFA  
238 method and its reproducibility. Consistent with previous studies,<sup>14,19</sup> we observed increased  
239 coherence in both groups during SSMs compared with the supine position in the VLF and LF  
240 ranges. This high coherence is usually indicative of the reliability of the assessed dCA  
241 indices. Additionally, the benefit of an additional dCA measurement during SSMs was found,  
242 which increased the specificity (91.67% vs. 79.17%). This could facilitate the identification  
243 of patients at risk of CH. However, there were no significance between-group differences in  
244 gain and absolute gain. One explanation for this may be that the phase is determined from the  
245 time delay between BP and CBF, and hence, is insensitive to any amplitude scaling.<sup>20</sup>  
246 Moreover, the phase is less sensitive to missing data than the gain and is reportedly a more  
247 reliable measure of dCA in clinical studies.<sup>21-23</sup> Another explanation may be that we included

248 a high proportion of patients with asymptomatic carotid artery stenosis, in whom dCA was  
249 not severely impaired.

250 Previous studies have investigated the predictive utility of changes in the PSV of the  
251 MCA on the surgical side at de-clamping,<sup>5</sup> postoperative increase ratio of the MCA<sup>24</sup>, and  
252 velocity BP index<sup>25</sup> for CHS. We focused on extracranial carotid hemodynamics and found  
253 that the  $PSV_{sten}/PSV_{dis}$  ratio was an independent predictor of CH, attributable to the negative  
254 association between the PSV ratio and cerebral perfusion. Previous research indicated that  
255 higher of  $PSV_{sten}/PSV_{dis}$  ratios are associated with severe stenosis<sup>26,27</sup>. Several recent studies  
256 have confirmed that severe carotid artery stenosis is a risk factor for CHS.<sup>2,28,29</sup> One study  
257 found a significantly higher incidence of hyperperfusion-induced intracranial hemorrhage  
258 after carotid artery stenting in patients with near-total occlusion than in those without (10.1%  
259 vs 0%).<sup>28</sup> Patients with severe unilateral carotid stenosis ( $\geq 90\%$ ) have a higher risk of  
260 hyperperfusion-induced intracranial hemorrhage after carotid artery stenting than those with  
261 less severe stenosis. According to Fan et al., the CH risk in patients with near-total occlusion  
262 had a 6.3-fold higher than that in patients with less severe stenosis.<sup>29</sup> The PSV ratio offers a  
263 more accurate and steadier parameter than arterial flow velocity measurement, which is  
264 affected by the presence of hypertension, hypotension, cardiac insufficiency, anemia,  
265 hyperthyroidism, and other diseases.<sup>30</sup> However, the presence of calcified atherosclerotic  
266 plaques and near-total occlusions may affect the prediction accuracy.<sup>31</sup>

267 Regarding the frequency domain of the dCA, we chose a VLF range of SSMs (0.02–  
268 0.07 Hz), considered to reflect the most relevant real-time dynamic dCA behavior.<sup>32</sup> The  
269  $PSV_{sten}/PSV_{dis}$  and phase degree of the MCA reflect extracranial hemodynamic and cerebral  
270 autoregulation. Both parameters are safe, cost-effective, and easy to use. Herein, the  
271 incidence of CHS after CEA was 2.2%; further, 11.1% of patients with CH developed CHS.

272 Prediction seeks to improve prompt interventions, which help prevent adverse events.

273 Accordingly, BP was more strictly controlled in patients at high risk for CHS. This might  
274 have reduced the occurrence of CHS and underestimated the positive predictive value of our  
275 index. In the present study, the addition of preoperative hemodynamic parameters did not  
276 improve the predictive value of dCA for CH after CEA. However, given the small number of  
277 patients with CHS, further studies on the mechanism underlying CHS are warranted.

278 This study has some limitations. First, this was a single-center study conducted in a  
279 university hospital setting, with a small sample size given the low incidence of CHS.  
280 Therefore, large-scale prospective studies in different settings are warranted to validate our  
281 findings. Second, we enrolled more men than women. Stroke and carotid artery stenosis are  
282 more common in men than in women<sup>33</sup>; moreover, there is a higher proportion of women  
283 with a poor temporal window than men. Third, TCD can only measure the velocity, not the  
284 flow volume. However, an MR angiography study reported that the MCA diameter did not  
285 significantly change in response to arterial pressure and CO<sub>2</sub> changes.<sup>34,35</sup> Therefore, the  
286 measured velocity is equivalent to the flow volume.

287

## 288 **Conclusions**

289 This study identified the lower ipsilateral phase as a predictor of CH after CEA. Impaired  
290 dCA may serve as a novel predictive tool for identifying patients who are at high risk of  
291 developing CH after CEA.

292

## 293 **List of Abbreviations**

294 aOR, adjusted odds ratio; AUC, area under the curve; BP, blood pressure; CBF, cerebral  
295 blood flow; CBFV, cerebral blood flow velocity; CEA, carotid endarterectomy; CH, cerebral  
296 hyperperfusion; CHS, cerebral hyperperfusion syndrome; CI, confidence interval; dCA,  
297 dynamic cerebral autoregulation; EDV, end diastolic velocity; Et-CO<sub>2</sub>, end-tidal carbon

298 dioxide; HF, high frequency; ICH, intracranial hemorrhage; LF, low frequency; MCA, middle  
299 cerebral artery; MCAV<sub>mea</sub>, mean flow velocity in the middle cerebral artery; NIBP, non-  
300 invasive continuous beat-to-beat BP; PI, pulsatility index; PI<sub>con</sub>, contralesional; PI<sub>oper</sub>,  
301 ipsilateral; PSV, peak systolic velocity; ROC, receiver operating characteristic; SSM, squat-  
302 stand maneuver; TCD, transcranial Doppler ultrasound; TFA, transfer function analysis; VLF,  
303 very low frequency

304

### 305 **Acknowledgements**

306 We thank the staff associated with the study and all the patients and their families for their  
307 cooperation. We would also thank Dr. Liyang Bao for his contribution to drawing figures.  
308 Figure 2 in the manuscript was drawn by Figdraw.

309

### 310 **Funding sources:**

311 This work was supported by Xuanwu Hospital Science Program for Fostering Young  
312 Scholars (Grant No. QNPY 2020021) And Beijing Hospitals Authority Youth Programme  
313 (code: QML20230814).

314

315

316 **Declarations of interest:** none

317

### 318 **References**

- 319 1. van Mook WN, Rennenberg RJ, Schurink GW, et al. Cerebral hyperperfusion syndrome.  
320 *Lancet Neurol.* 2005;4:877-888. [https://doi.org/10.1016/S1474-4422\(05\)70251-9](https://doi.org/10.1016/S1474-4422(05)70251-9).
- 321 2. Lin YH, Liu HM. Update on cerebral hyperperfusion syndrome. *J Neurointerv Surg.*  
322 2020;12:788-793. <https://doi.org/10.1136/neurintsurg-2019-015621>.
- 323 3. Kirchoff-Torres KF, Bakradze E. Cerebral hyperperfusion syndrome after carotid



- 324 revascularization and acute ischemic stroke. *Curr Pain Headache Rep.* 2018;22:24.  
325 <https://doi.org/10.1007/s11916-018-0678-4>.
- 326 4. Ogasawara K, Sakai N, Kuroiwa T, et al. Intracranial hemorrhage associated with cerebral  
327 hyperperfusion syndrome following carotid endarterectomy and carotid artery  
328 stenting: retrospective review of 4494 patients. *J Neurosurg.* 2007;107:1130-1136.  
329 <https://doi.org/10.3171/JNS-07/12/1130>.
- 330 5. Dalman JE, Beenackers IC, Moll FL, Leusink JA, Ackerstaff RG. Transcranial doppler  
331 monitoring during carotid endarterectomy helps to identify patients at risk of  
332 postoperative hyperperfusion. *Eur J Vasc Endovasc Surg.* 1999;18:222-227.  
333 <https://doi.org/10.1053/ejvs.1999.0846>.
- 334 6. Xiong L, Liu X, Shang T, et al. Impaired cerebral autoregulation: measurement and  
335 application to stroke. *J Neurol Neurosurg Psychiatry.* 2017;88:520-531.  
336 <https://doi.org/10.1136/jnnp-2016-314385>.
- 337 7. Claassen JA, Meel-van den Abeelen AS, Simpson DM, Panerai RB, international Cerebral  
338 Autoregulation Research Network (CARNet). Transfer function analysis of dynamic  
339 cerebral autoregulation: a white paper from the international cerebral autoregulation  
340 research network. *J Cereb Blood Flow Metab.* 2016;36:665-680.  
341 <https://doi.org/10.1177/0271678X15626425>.
- 342 8. Xiong L, Tian G, Lin W, et al. Is dynamic cerebral autoregulation bilaterally impaired after  
343 unilateral acute ischemic stroke? *J Stroke Cerebrovasc Dis.* 2017;26:1081-1087.  
344 <https://doi.org/10.1016/j.jstrokecerebrovasdis.2016.12.024>.
- 345 9. Oeinck M, Neunhoeffler F, Buttler KJ, et al. Dynamic cerebral autoregulation in acute  
346 intracerebral hemorrhage. *Stroke.* 2013;44:2722-2728.  
347 <https://doi.org/10.1161/STROKEAHA.113.001913>.
- 348 10. Indelicato E, Fanciulli A, Poewe W, Antonini A, Pontieri FE, Wenning GK. Cerebral

- 349 autoregulation and white matter lesions in Parkinson's disease and multiple system  
350 atrophy. *Parkinsonism Relat Disord*. 2015;21:1393-1397.  
351 <https://doi.org/10.1016/j.parkreldis.2015.10.018>.
- 352 11. Kneihsl M, Hinteregger N, Nistl O, et al. Post-reperfusion hyperperfusion after  
353 endovascular stroke treatment: a prospective comparative study of TCD versus MRI.  
354 *J NeuroIntervent Surg*. 2022; neurintsurg-2022-019213. [https://doi.org/10.1136/jnis-](https://doi.org/10.1136/jnis-2022-019213)  
355 [2022-019213](https://doi.org/10.1136/jnis-2022-019213).
- 356 12. Barnett HJ, Taylor DW, Eliasziw M, et al. Benefit of carotid endarterectomy in patients  
357 with symptomatic moderate or severe stenosis. North American Symptomatic Carotid  
358 Endarterectomy Trial Collaborators. *N Engl J Med*. 1998;339:1415-1425.  
359 <https://doi.org/10.1056/NEJM199811123392002>.
- 360 13. Zhang R, Zuckerman JH, Iwasaki K, Wilson TE, Crandall CG, Levine BD. Autonomic  
361 neural control of dynamic cerebral autoregulation in humans. *Circulation*.  
362 2002;106:1814-1820. <https://doi.org/10.1161/01.cir.0000031798.07790.fe>.
- 363 14. Junejo RT, Braz ID, Lucas SJ, et al. Neurovascular coupling and cerebral autoregulation  
364 in atrial fibrillation. *J Cereb Blood Flow Metab*. 2020;40:1647-1657.  
365 <https://doi.org/10.1177/0271678X19870770>.
- 366 15. Batterham AP, Panerai RB, Robinson TG, Haunton VJ. Does depth of squat-stand  
367 maneuver affect estimates of dynamic cerebral autoregulation? *Physiol Rep*.  
368 2020;8:e14549. <https://doi.org/10.14814/phy2.14549>.
- 369 16. Zhang R, Zuckerman JH, Giller CA, Levine BD. Transfer function analysis of dynamic  
370 cerebral autoregulation in humans. *Am J Physiol*. 1998;274:H233-H241.  
371 <https://doi.org/10.1152/ajpheart.1998.274.1.h233>.
- 372 17. Chen Y, Song G, Jiao L, Wang Y, Ma Y, Ling F. A study of carotid endarterectomy in a  
373 Chinese population: initial experience at a single center. *Clin Neurol Neurosurg*.

- 374 2014;126:88-92. <https://doi.org/10.1016/j.clineuro.2014.08.025>.
- 375 18. Fassaert LMM, Immink RV, van Vriesland DJ, et al. Transcranial doppler 24 hours after  
376 carotid endarterectomy accurately identifies patients not at risk of cerebral  
377 hyperperfusion syndrome. *Eur J Vasc Endovasc Surg*. 2019;58:320-327.  
378 <https://doi.org/10.1016/j.ejvs.2019.04.033>.
- 379 19. Claassen JA, Levine BD, Zhang R. Dynamic cerebral autoregulation during repeated  
380 squat-stand maneuvers. *J Appl Physiol (1985)*. 2009;106:153-160.  
381 <https://doi.org/10.1152/jappphysiol.90822.2008>.
- 382 20. Panerai RB, Brassard P, Burma JS, Castro P, Claassen JA, van Lieshout JJ, et al. Transfer  
383 function analysis of dynamic cerebral autoregulation: a CARNet white paper 2022  
384 update. *J Cereb Blood Flow Metab*. 2023; 43:3-25.
- 385 21. Deegan BM, Serrador JM, Nakagawa K, Jones E, Sorond FA, O'laighin G. The effect of  
386 blood pressure calibrations and transcranial doppler signal loss on transfer function  
387 estimates of cerebral autoregulation. *Med Eng Phys*. 2011;33:553-562.  
388 <https://doi.org/10.1016/j.medengphy.2010.12.007>.
- 389 22. Intharakham K, Beishon L, Panerai RB, Haunton VJ, Robinson TG. Assessment of  
390 cerebral autoregulation in stroke: a systematic review and meta-analysis of studies at  
391 rest. *J Cereb Blood Flow Metab*. 2019;39:2105-2116.  
392 <https://doi.org/10.1177/0271678X19871013>.
- 393 23. Sheriff F, Castro P, Kozberg M, et al. Dynamic cerebral autoregulation post endovascular  
394 thrombectomy in acute ischemic stroke. *Brain Sci*. 2020;10:641.  
395 <https://doi.org/10.3390/brainsci10090641>.
- 396 24. Li QP, Hua Y, Liu JB, et al. Intraoperative transcranial Doppler monitoring predicts the  
397 risk of cerebral hyperperfusion syndrome after carotid endarterectomy. *World*  
398 *Neurosurg*. 2022;165:e571-e580. <https://doi.org/10.1016/j.wneu.2022.06.100>.

- 399 25. Lai ZC, Liu B, Chen Y, Ni L, Liu CW. Prediction of cerebral hyperperfusion syndrome  
400 with velocity blood pressure index. *Chin Med J (Engl)*. 2015;128:1611-1617.  
401 <https://doi.org/10.4103/0366-6999.158317>.
- 402 26. Soulez G, Therasse E, Robillard P, et al. The value of internal carotid systolic velocity  
403 ratio for assessing carotid artery stenosis with Doppler sonography. *AJR Am J*  
404 *Roentgenol*. 1999;Jan;172:207-212. <https://doi.org/10.2214/ajr.172.1.9888769>.
- 405 27. Ranke C, Creutzig A, Becker H, Trappe HJ. Standardization of carotid ultrasound: a  
406 hemodynamic method to normalize for interindividual and interequipment variability.  
407 *Stroke*. 1999;Feb;30:402-406. <https://doi.org/10.1161/01.str.30.2.402>.
- 408 28. Zhang L, Dai D, Li Z, et al. Risk factors for hyperperfusion-induced intracranial  
409 hemorrhage after carotid artery stenting in patients with symptomatic severe carotid  
410 stenosis evaluation. *J Neurointerv Surg*. 2019;11:474-478.  
411 <https://doi.org/10.1136/neurintsurg-2018-013998>.
- 412 29. Fan X, Lai Z, Lin T, et al. Multidelay MR arterial spin labeling perfusion map for the  
413 prediction of cerebral hyperperfusion after carotid endarterectomy. *J Magn Reson*  
414 *Imaging*. 2023;58:1245-1255. <https://doi.org/10.1002/jmri.28634>.
- 415 30. The Professional Committee of Vascular Ultrasound of Stroke Prevention and Treatment  
416 Expert, Committee of the National Health Commission, The Professional Committee  
417 of Superficial Organ and Peripheral Vascular Ultrasound of the Chinese Medical  
418 Ultrasound Engineering, The Professional Committee of Craniocerebral and Cervical  
419 Vascular Ultrasound of the Chinese Medical Ultrasound Engineering. Expert  
420 consensus on some issues of cerebral and carotid vascular ultrasonography. *Adv*  
421 *Ultrasound Diagn Ther*. 2021;02:153-162.  
422 <https://doi.org/10.37015/AUDT.2021.200057>.
- 423 31. Brouwers JJWM, Jiang JFY, Feld RT, et al. A New Doppler-Derived Parameter to

- 424 Quantify Internal Carotid Artery Stenosis: Maximal Systolic Acceleration. *Ann Vasc*  
425 *Surg.* 2022; 81:202-210. <https://doi.org/10.1016/j.avsg.2021.09.056>.
- 426 32. Haubrich C, Wendt A, Diehl RR, Klötzsch C. Dynamic autoregulation testing in the  
427 posterior cerebral artery. *Stroke.* 2004;35:848-852.  
428 <https://doi.org/10.1161/01.STR.0000120729.99039.B6>.
- 429 33. Bonati LH, Jansen O, de Borst GJ, Brown MM. Management of atherosclerotic  
430 extracranial carotid artery stenosis. *Lancet Neurol.* 2022;21:273-283.  
431 [https://doi.org/10.1016/S1474-4422\(21\)00359-8](https://doi.org/10.1016/S1474-4422(21)00359-8).
- 432 34. Serrador JM, Picot PA, Rutt BK, Shoemaker JK, Bondar RL. MRI measures of middle  
433 cerebral artery diameter in conscious humans during simulated orthostasis. *Stroke.*  
434 2000;31:1672-1678. <https://doi.org/10.1161/01.str.31.7.1672>.
- 435 35. Verbree J, Bronzwaer AS, Ghariq E, et al. Assessment of middle cerebral artery diameter  
436 during hypocapnia and hypercapnia in humans using ultra-high-field MRI. *J Appl*  
437 *Physiol (1985).* 2014;117:1084-1089.  
438 <https://doi.org/10.1152/jappphysiol.00651.2014>.

439

#### 440 **Figure legends**

441 **Figure 1** Flowchart of patient enrollment

442

443 **Figure 2** The study protocol.

444 All the enrolled patients received dCA measurement before carotid endarterectomy. The dCA  
445 measurement included supine position (10 min), standing (2 min), and squat-stand maneuvers  
446 (5 min).

447

448 **Figure 3** Between-model comparisons of ROC curves for predicting the outcome.  
449 Model 1: the ipsilateral phase (supine) at very low frequency, *dark purple line*. Model 2: the  
450 ipsilateral phase (SSMs) at very low frequency, *green line*. Model 3: Model 1 +  
451  $PSV_{sten}/PSV_{dis}$ , *orange line*. Model 4: Model 2 +  $PSV_{sten}/PSV_{dis}$ , *green dotted line*.  
452 PSV, peak systolic velocity; ROC, receiver operating characteristics; SSMs, squat-stand  
453 maneuvers

454  
455 **Figure 4** Number of patients according to different cut-off values of ipsilateral phase.  
456 (a) The proportion of patients with CH in the ipsilateral phase (supine)  $\leq 24.7$  group was  
457 significantly higher than that in the ipsilateral phase (supine)  $> 24.7$  group (50.0% vs. 5.0%,  
458  $P < 0.001$ ). (b) The proportion of patients with CH in the ipsilateral phase (SSMs)  $\leq 11.7$   
459 group was significantly higher than that in the ipsilateral phase (SSMs)  $> 11.7$  group (68.4%  
460 vs. 7.0%,  $P < 0.001$ )  
461 CH, cerebral hyperperfusion; SSMs, squat-stand maneuvers

462

463

464

465

**Table 1.** Clinical characteristics and hemodynamic parameters.

Characteristic	All(n=90)	CH(n=18)	Non-CH(n=72)	<i>P</i>
<b>Demographic variables</b>				
Age,years	63.1±7.6	61.8±6.6	63.5±7.8	0.395
Male	82(91.1)	15(83.3)	67(93.1)	0.195
BMI	25.0±2.7	24.7±2.6	25.0±2.7	0.643
<b>Vascular risk factors</b>				
Hypertension	61(67.8)	15(83.3)	46(63.9)	0.160
Diabetes mellitus	34(37.8)	8(44.4)	26(36.1)	0.514
hyperlipidemia	46(51.1)	10(55.6)	36(50.0)	0.673
coronary artery disease	19(21.1)	3(16.7)	16(22.2)	0.754
smoking	66(73.3)	14(77.8)	52(72.2)	0.771
alcohol	48(53.3)	10(55.6)	38(52.8)	0.833
<b>Laboratory indexes</b>				
Serum triglycerides, mmol/L	1.3(0.9-1.6)	1.3(0.9-1.8)	1.3(0.9-1.6)	0.646
Total cholesterol, mmol/L	3.4(3.0-4.1)	3.2(2.9-3.6)	3.5(3.1-4.2)	0.195
High-density lipoprotein, mmol/L	1.0(0.8-1.1)	0.9(0.8-1.1)	1.0(0.8-1.2)	0.293
Low-density lipoprotein, mmol/L	1.9(1.5-2.4)	1.7(1.5-2.1)	1.9(1.5-2.5)	0.385
<b>Hemodynamic parameters</b>				
PSV <sub>sten</sub> / PSV <sub>dis</sub>	7.9(5.7-14.1)	17.3(12.3-32.3)	7.1(5.4-11.0)	< 0.001
PI <sub>con</sub> /PI <sub>oper</sub>	1.4(1.2-1.5)	1.5(1.2-1.6)	1.3(1.2-1.5)	0.092
<b>Presence of primary collaterals</b>	79(87.8)	14(77.8)	65(90.3)	0.220

<b>Operation side, right</b>	51(56.7)	13(72.2)	38(52.8)	0.136
<b>Post-operative imaging</b>				
asymptomatic acute embolic lesions	9(10)	1(5.6)	8(11.1)	0.102
hemorrhagic complications	1(11.1)	1(5.6)	0	

BMI: body mass index;  $PSV_{sten}/PSV_{dis}$ : ratio of peak systolic velocity at the carotid stenosis to peak systolic velocity at 4–6 cm beyond the carotid bifurcation;  $PI_{con}/PI_{oper}$ : ratio of the pulsatility index of the ipsilateral middle cerebral artery to the pulsatility index of the contralesional middle cerebral artery; Presence of primary collaterals: anterior communicating artery and/or posterior communicating artery appearing on computed tomography angiography or magnetic resonance angiography images.

**Table 2.** Cerebral autoregulation parameters before endarterectomy during the supine position.

Frequency	Parameters	CH(n=18)	Non-CH(n=72)	<i>P</i>
VLF	phase (degree)			
	<b>ipsilateral</b>	<b>18.29(8.34-24.57)</b>	<b>42.12(30.16-55.91)</b>	<b>&lt; 0.001</b>
	contralateral	47.01(27.17-65.97)	51.15(40.01-69.41)	0.242
	gain [cm/ (s·mm Hg)]			
	ipsilateral	0.60(0.46-0.93)	0.64(0.48-0.84)	0.844
	contralateral	0.71(0.57-0.93)	0.73(0.61-0.97)	0.657
	gain (%/mm Hg)			



	ipsilateral	1.04(0.76-1.33)	1.04(0.85-1.29)	0.996
	contralateral	1.01(0.73-1.21)	1.10(0.87-1.38)	0.071
	coherence			
	ipsilateral	0.80(0.75-0.87)	0.69(0.64-0.74)	< 0.001
	contralateral	0.70(0.65-0.78)	0.67(0.64-0.73)	0.157
LF	phase (degree)			
	<b>ipsilateral</b>	<b>13.31(4.50-24.20)</b>	<b>31.45(17.12-42.08)</b>	<b>0.001</b>
	contralateral	25.96(14.87-43.53)	37.98(27.73-51.31)	0.076
	gain [cm/ (s·mm Hg)]			
	ipsilateral	0.57(0.39-0.83)	0.68(0.56-0.86)	0.131
	contralateral	0.80(0.67-0.91)	0.91(0.66-1.09)	0.299
	gain (%/mm Hg)			
	ipsilateral	0.97(0.75-1.22)	1.15(0.92-1.51)	0.056
	contralateral	1.15(0.95-1.32)	1.28(1.03-1.65)	0.074
	coherence			
	ipsilateral	0.72(0.68-0.77)	0.68(0.64-0.76)	0.327
	contralateral	0.70(0.64-0.74)	0.70(0.64-0.74)	0.801
HF	phase (degree)			
	ipsilateral	27.97(8.20-47.37)	20.15(12.18-29.20)	0.105
	contralateral	22.28(12.20-35.45)	19.40(10.13-28.26)	0.276
	gain [cm/ (s·mm Hg)]			
	ipsilateral	0.54(0.38-0.73)	0.61(0.45-0.82)	0.250

	contralateral	0.69(0.60-0.94)	0.81(0.67-1.06)	0.119
	gain (%/mm Hg)			
	ipsilateral	0.89(0.61-1.19)	1.04(0.78-1.35)	0.153
	contralateral	1.03(0.92-1.25)	1.17(1.00-1.44)	0.069
	coherence			
	ipsilateral	0.76(0.71-0.79)	0.74(0.69-0.79)	0.697
	contralateral	0.74(0.68-0.78)	0.75(0.70-0.79)	0.374
Et-CO <sub>2</sub>		38.1±2.1	38.5±2.0	0.395

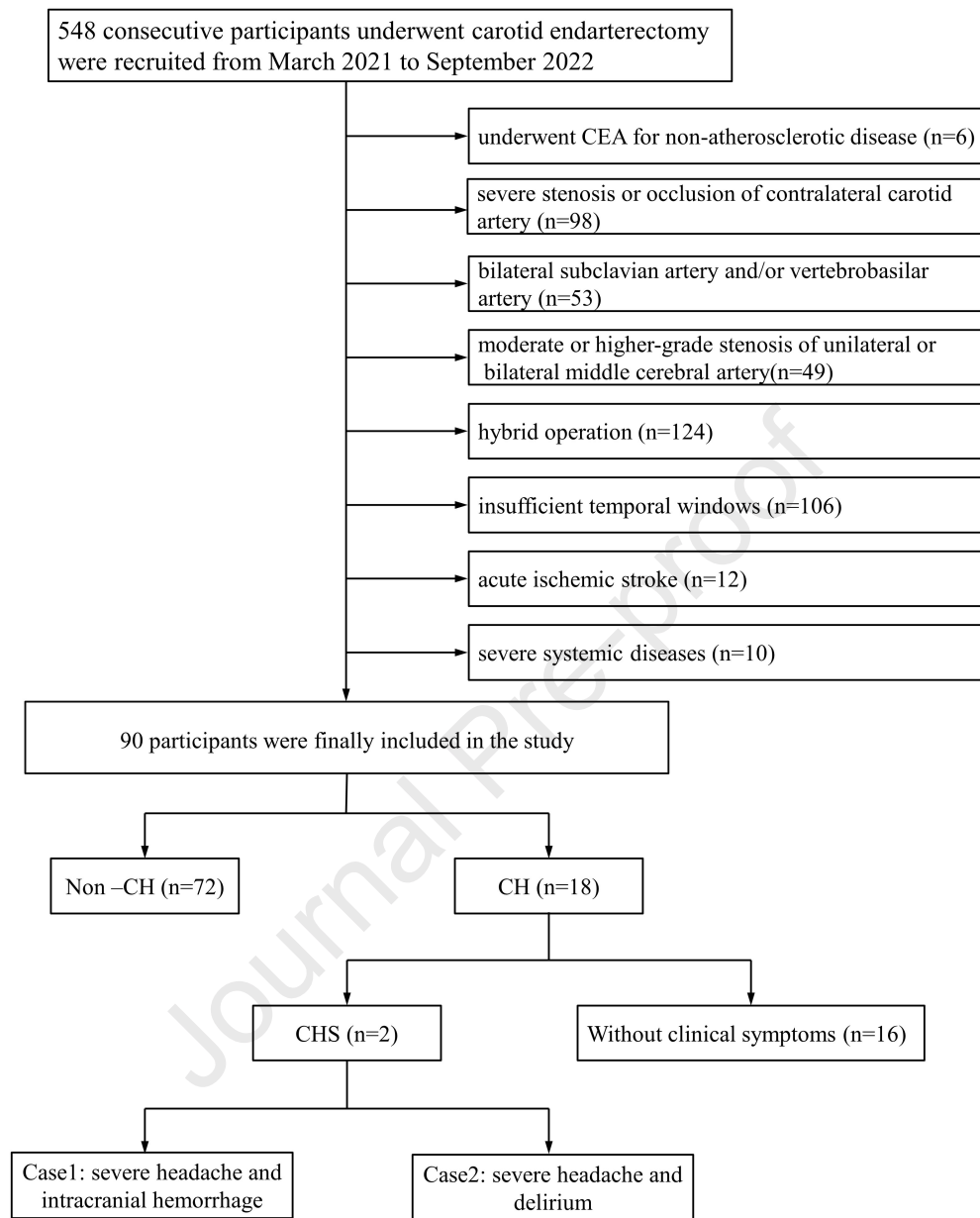
VLF: very low frequency; LF: low frequency; HF: high frequency; Et-CO<sub>2</sub>: end-tidal carbon dioxide.

**Table 3.** Cerebral autoregulation parameters before endarterectomy during squat-stand maneuvers.

Frequency	Parameters	CH(n=18)	Non-CH(n=72)	<i>P</i>
VLF	phase (degree)			
	<b>ipsilateral</b>	<b>9.36(6.39-25.25)</b>	<b>34.04(23.14-51.27)</b>	<b>&lt; 0.001</b>
	contralateral	49.32(32.31-65.07)	46.13(36.31-58.06)	0.840
	gain [cm/ (s·mm Hg)]			
	ipsilateral	0.65(0.41-0.74)	0.59(0.50-0.81)	0.690
	contralateral	0.68(0.54-0.89)	0.70(0.56-0.97)	0.900
	gain (%/mm Hg)			
	ipsilateral	1.09(0.97-1.35)	1.13(0.96-1.47)	0.657
	contralateral	0.98(0.89-1.16)	1.13(0.91-1.46)	0.105
	coherence			
ipsilateral	0.93(0.88-0.95)	0.91(0.86-0.94)	0.223	
contralateral	0.89(0.75-0.91)	0.91(0.87-0.94)	0.056	
LF	phase (degree)			

	<b>ipsilateral</b>	<b>7.69(4.04-20.55)</b>	<b>22.12(14.07-29.49)</b>	<b>0.001</b>
	contralateral	23.88(16.85-40.59)	29.49(20.60-40.45)	0.455
	gain [cm/ (s·mm Hg)]			
	ipsilateral	0.61(0.43-0.83)	0.77(0.56-0.91)	0.095
	contralateral	0.84(0.70-1.21)	0.97(0.76-1.21)	0.372
	gain (%/mm Hg)			
	ipsilateral	1.08(0.79-1.36)	1.28(1.03-1.65)	0.119
	contralateral	1.20(0.97-1.47)	1.41(1.13-1.64)	0.063
	coherence			
	ipsilateral	0.79(0.72-0.81)	0.78(0.72-0.84)	0.720
	contralateral	0.74(0.66-0.83)	0.78(0.73-0.83)	0.248
HF	phase (degree)			
	ipsilateral	22.96(11.67-28.74)	16.18(9.16-21.64)	0.146
	contralateral	17.78(7.27-22.10)	17.53(12.26-25.75)	0.545
	gain [cm/ (s·mm Hg)]			
	ipsilateral	0.58(0.39-0.79)	0.65(0.53-0.79)	0.323
	contralateral	0.86(0.58-1.33)	0.90(0.66-1.14)	0.880
	gain (%/mm Hg)			
	ipsilateral	1.09(0.67-1.26)	1.21(0.98-1.41)	0.386
	contralateral	1.20(0.91-1.50)	1.31(1.12-1.77)	0.101
	coherence			
	ipsilateral	0.74(0.68-0.77)	0.74(0.67-0.80)	0.603
	contralateral	0.75(0.66-0.78)	0.75(0.68-0.82)	0.470
	Et-CO <sub>2</sub>	38.6±1.9	38.2±2.0	0.494

VLF: very low frequency; LF: low frequency; HF: high frequency; Et-CO<sub>2</sub>: end-tidal carbon dioxide.

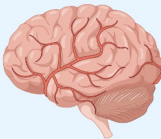


population

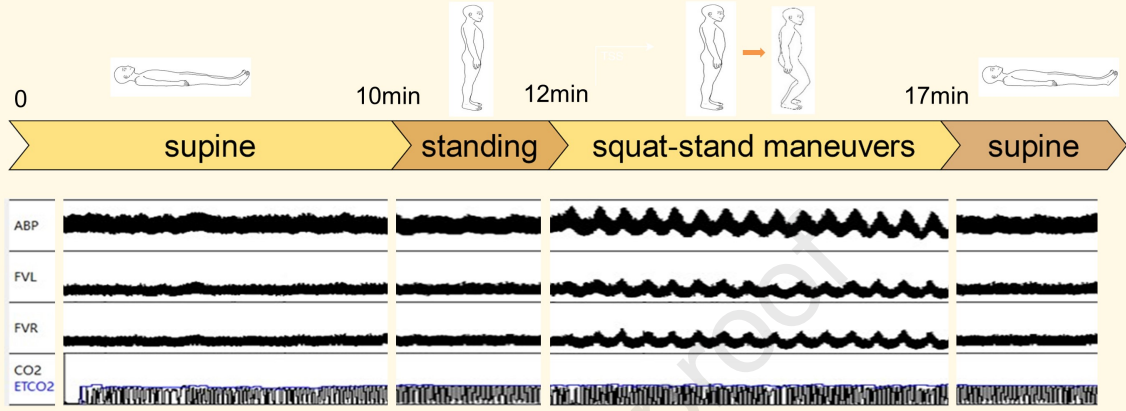
90 patients with unilateral severe carotid artery stenosis

91% Male

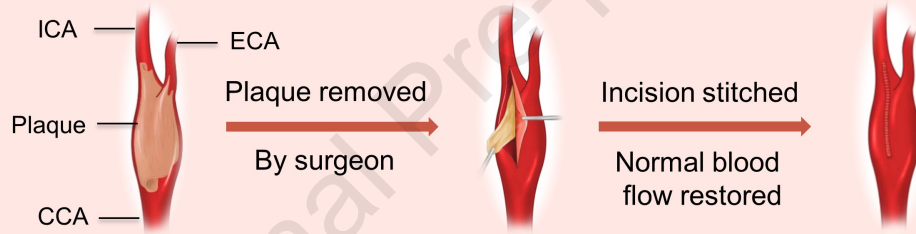
63 Mean age

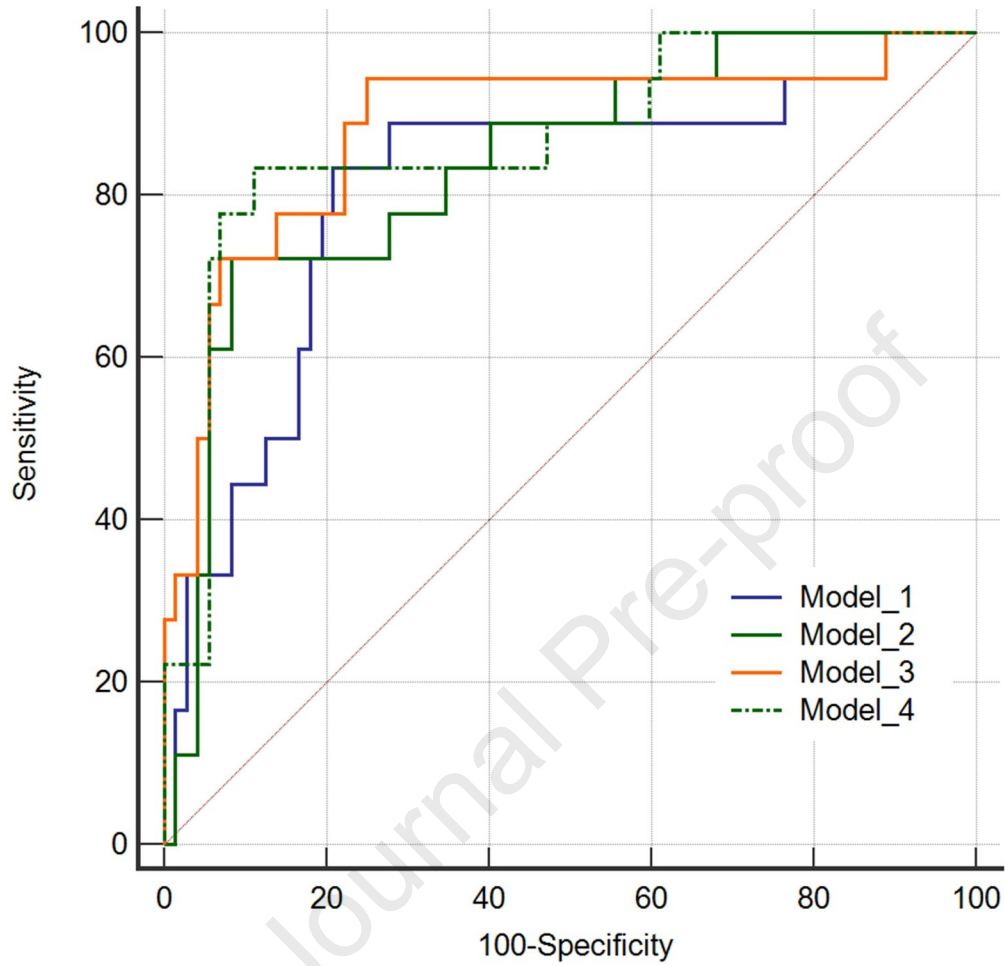


dCA measurement

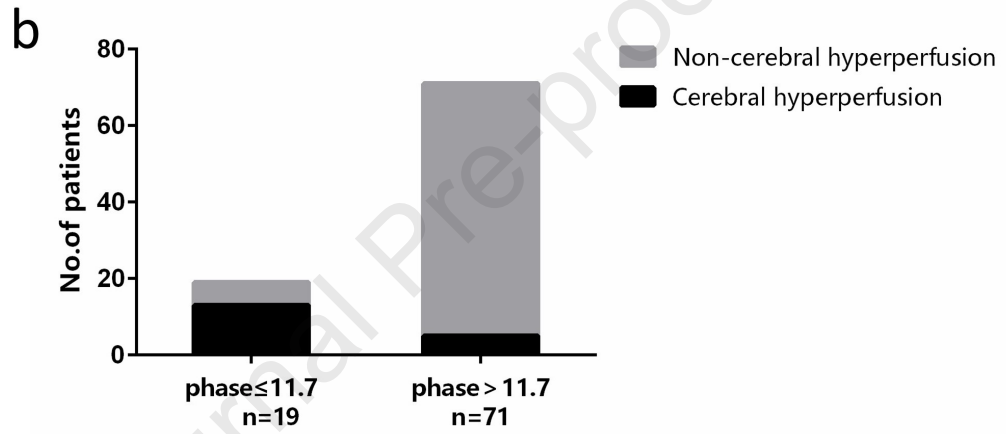
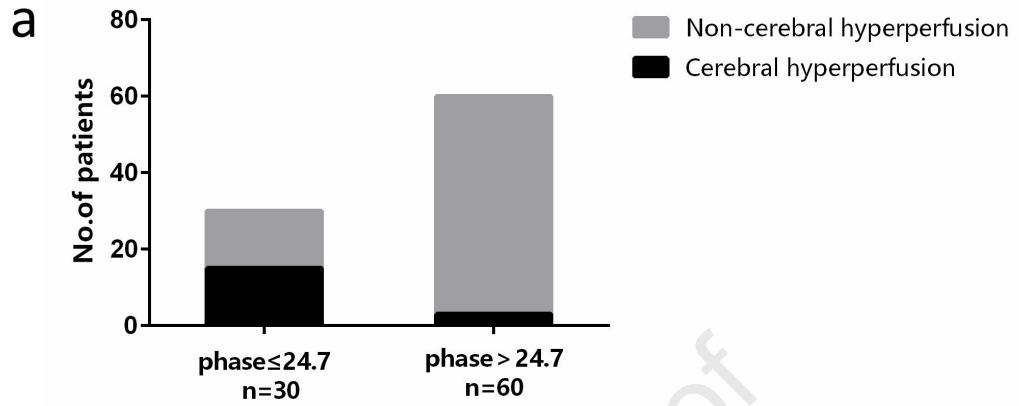


CEA





	AUC	95%CI	sensitivity	specificity
Model 1	0.809	0.712-0.884	83.33%	79.17%
Model 2	0.839	0.746-0.908	72.22%	91.67%
Model 3	0.883	0.799-0.942	94.44%	75.0%
Model 4	0.869	0.781-0.931	83.33%	88.89%



**List of Abbreviations**

aOR, adjusted odds ratio; AUC, area under the curve; BP, blood pressure; CBF, cerebral blood flow; CBFV, cerebral blood flow velocity; CEA, carotid endarterectomy; CH, cerebral hyperperfusion; CHS, cerebral hyperperfusion syndrome; CI, confidence interval; dCA, dynamic cerebral autoregulation; EDV, end diastolic velocity; Et-CO<sub>2</sub>, end-tidal carbon dioxide; HF, high frequency; ICH, intracranial hemorrhage; LF, low frequency; MCA, middle cerebral artery; MCAV<sub>mea</sub>, mean flow velocity in the middle cerebral artery; NIBP, non-invasive continuous beat-to-beat BP; PI, pulsatility index; PIcon, contralesional; POper, ipsilateral; PSV, peak systolic velocity; ROC, receiver operating characteristic; SSM, squat-stand maneuver; TCD, transcranial Doppler ultrasound; TFA, transfer function analysis; VLF, very low frequency



**Declaration of interests**

The authors declare that they have no known competing financial interests or personal relationships that could have appeared to influence the work reported in this paper.

The authors declare the following financial interests/personal relationships which may be considered as potential competing interests:

Journal Pre-proof

**Author statement**

**Na Li:** Conceptualization, Data curation, Formal analysis, Methodology, Writing – original draft. **Fubo Zhou:** Data curation, Formal analysis, Writing – review & editing. **Xia Lu:** Data curation, Writing – review & editing. **Hongxiu Chen:** Data curation, Methodology, Writing – review & editing. **Ran Liu:** Data curation, Methodology, Writing – review & editing. **Songwei Chen:** Data curation, Methodology, Writing – review & editing. **Yingqi Xing:** Project administration, Investigation, Methodology, Writing – review & editing.